[28]M. H. Jericho and A. M. Simpson, Phil. Mag. 17, 267 (1968).
[29]G. A. Baraff and T. G. Phillips, Phys. Rev. Letters 24, 1428 (1970).
[30]T. G. Phillips, G. A. Baraff, and P. H. Schmidt, Phys. Rev. B 5, 1283 (1972).

PHYSICAL REVIEW B VOLUME 6, NUMBER 4 15 AUGUST 1972

Energy Dependence of the Effective Debye Temperature Obtained from Low-Energy–Electron-Diffraction-Intensity Measurements*

G. E. Laramore
Sandia Laboratories, Albuquerque, New Mexico 87115
(Received 11 February 1972)

A discussion of the effect of lattice vibrations on the effective electron–ion-core elastic scattering vertex is given using the model of Duke and Laramore. The renormalization introduced by the lattice vibrations can substantially increase the number of partial waves necessary to describe this scattering. The vertex approximation using the s-wave part of the phonon renormalization factor and phase shifts from a realistic potential to describe the electron–rigid-ion scattering is compared with the vertex approximation using the full phonon renormalization factor and the constant phase shift s-wave model to describe the electron–rigid-ion scattering. Model calculations of low-energy–electron-diffraction (LEED) intensity profiles are presented for a system having the geometrical parameters of Al(100), and effective Debye temperatures are obtained for the Bragg peaks in the intensity profiles. The dependence of these effective Debye temperatures on the ineleastic-collision mean free path and on the characteristic falloff of the vibrational amplitude of the ion cores with distance from the surface is investigated. Even for a constant mean free path the Θ_D^{eff} exhibit a pronounced energy dependence. By comparing the calculated Θ_D^{eff} with the experimental measurements of Quinto *et al.*, a crude estimate of the inelastic-collision mean free path in the surface region of aluminum is obtained.

I. INTRODUCTION

It is well known that lattice vibrations introduce a temperature dependence into the intensities of x rays[1] and neutrons[2] scattered by a solid. Since the x rays and neutrons interact only weakly with the ion cores of the solid, their scattering can be treated in linear response theory and so the temperature dependence of the scattered beams can be simply related to a Debye temperature[3] which characterizes the vibrational amplitudes of the ion cores in the "bulk" region of the solid. Low-energy electrons, on the other hand, interact quite strongly with the ion cores of the solid and also with the high-energy electronic excitations (e.g., plasmons, interband transitions). These effects greatly complicate the interpretation of the temperature dependence of the elastic scattering intensity for electrons.[4,5] However, it is an experimental fact that the temperature dependence of the intensity of maxima in low-energy–electron-diffraction (LEED) intensity profiles can be described in terms of an effective Debye temperature.[6–15] A common feature of these observations is that in a given intensity profile the low-energy maxima are characterized by a smaller effective Debye temperature Θ_D^{eff} than the higher-energy maxima. This smaller Θ_D^{eff} for the lower-energy peaks is indicative of a larger amplitude of vibration for the surface atoms than for those atoms in the "bulk" region of the solid. Duke and Laramore[4,5] investigated the consequences of lattice vibrations in a theoretical calculation of the LEED intensity profiles and showed that for the range of electron energies commonly used in LEED, their main effect was to renormalize the effective electron–ion-core elastic scattering vertex, making it temperature dependent. They investigated the effects of a vibronically inequivalent surface layer[5] on the temperature dependence of the elastic intensity profiles and showed that although the temperature dependence of the peaks in the intensity profiles could be described in terms of a Θ_D^{eff}, this effective Debye temperature could not be simply related to the vibrational amplitudes of either the surface or the bulk ion cores. The Θ_D^{eff} obtained from this analysis depends as well on the relative scattering strengths of the surface and bulk ion cores and upon the inelastic mean free path which determines the relative sampling of the surface and bulk regions of the elastic beam.

Recent model calculations[16–22] indicate that for a clean surface it is reasonable to use the same potential to describe the interaction between the beam electrons and both the surface and bulk ion cores of the solid. The rationale for this is that the electron

energies and experimental geometry used in LEED mean that large-angle scattering events dominate the features of the LEED intensity profiles. These scattering events involve large momentum transfers and hence probe the part of the electron–ion-core potential determined by the atomic core levels.[23,24] This part of the potential is not greatly affected by the local screening of the ion core and hence is the same whether the ion core is located on the surface of the material or in the bulk. Thus, for a clean material the "unknown" quantities on which a measurement of $\Theta_D^{\rm eff}(E)$ may shed some light are the imaginary part of the electronic self-energy $\mathrm{Im}\Sigma$ in the surface region and the vibrational amplitudes of the ion cores in the surface region. For a given model of $\mathrm{Im}\Sigma$ the data can be used to extract information about the vibronic properties of the surface atoms; or, conversely, for a given model of vibronic properties of the surface atoms, the data can be used to extract information about $\mathrm{Im}\Sigma$ in the surface region. Unfortunately, neither of these quantities is accurately known for the case of a metal and so it is necessary to determine both quantities in a self-consistent manner. Such a program would require analyzing a rather large block of LEED data over a wide range of temperatures, energies and angles and is outside the scope of the present paper. Here we merely wish to examine some of the features of LEED calculations which use different approximations for the renormalized electron–ion-core elastic scattering vertex.

The vibronic renormalization of the electron–ion-core elastic scattering vertex significantly alters the angular dependence of the vertex and this substantially increases the number of partial waves necessary to describe the vertex. One approach that has been taken[18] to avoid this difficulty is to accurately model the electron–rigid-ion-core portion of the vertex and use only the s-wave portion of the phonon renormalization factor. Although this procedure produces calculated intensity profiles that are in qualitative agreement with experimental data we shall see that it does not quantitatively describe the temperature dependence of the LEED intensity profiles. Another approach is to simply parametrize the electron–rigid-ion portion of the vertex in terms of the constant-phase-shift s-wave model[5,25,26] and then use the available partial waves to accurately model the vibronic renormalization factor. This procedure restricts our analysis to only the primary "Bragg" peaks[27] but it does seem to provide a reasonable description of the temperature dependence of their intensities.

We shall also see that although it is commonly thought that the energy dependence of $\Theta_D^{\rm eff}$ denotes an energy-dependent inelastic mean free path, this is not necessarily the case. Even for a constant inelastic mean free path, a significant energy dependence to $\Theta_D^{\rm eff}$ can occur when the vibrational amplitude of the surface atoms is much larger than those in the bulk. For such a case the effective vibrationally renormalized scattering cross section drops off much faster with increasing energy for the surface atoms than for the bulk atoms, and so with increasing electron energy the contribution to the LEED intensity of the surface atoms relative to the contribution of the bulk atoms decreases. This effect is evident in Tables III and IV of Ref. 5 although it is not emphasized there. This paper also augments the work of Laramore and Duke[5] in that rather than calculating the elastic scattering intensity using the double-diffraction approximation,[25] here we use the full-matrix-inversion method of solution.[26] We also investigate the effects of having more than one atomic layer in the surface region vibronically inequivalent to those in the bulk. By comparing the results of our calculations with the experimental measurements of Quinto *et al.*[28] on Al(100), we obtain a *crude* estimate of the effective inelastic mean free path and hence of $\mathrm{Im}\Sigma$ for this material. We consider only the "Bragg" peaks[27] of the intensity profiles. The $\Theta_D^{\rm eff}$ obtained for the $n=2$, 3, and 4 "Bragg" peaks by Quinto *et al.* are shown in Table I. These values were obtained using a kinematical analysis of the scattered intensity assuming a Debye model for the phonon spectrum of the solid in the temperature range 300–600 °K.

In Sec. II we review the models for the renormalized electron–ion-core elastic scattering vertex and for the electronic self-energy which are used in the calculation. In Sec. III, we present calculated intensity profiles and effective Debye temperatures using different models for the renormalized electron–ion-core elastic scattering vertex, and in Sec. IV we briefly summarize our results.

II. DEFINITION OF MODEL

The basic model used in this work has been extensively described elsewhere,[4,5,22] and so here we

TABLE I. Experimental effective Debye temperatures (Ref. 28) for the first three Bragg peaks for the (00) beam for Al(100).[a]

Peak	Energy (eV)	$\Theta_D^{\rm eff}$ (°K)
$n=2$ Bragg peak	26	189
$n=3$ Bragg peak	69	236
$n=4$ Bragg peak	134	331

[a]The incident beam makes an angle of 5° with the normal to the crystal face, and the scattering plane makes an angle of 5° with one of the cubic axes in the plane.

only review some of the salient features. The main effect of the lattice vibrations is to renormalize the effective electron–ion-core elastic scattering amplitude, making it temperature dependent. The renormalized scattering amplitude for the nth ion core is given by

$$b_n(\vec{k}_2, \vec{k}_1) = \exp[-\tfrac{1}{2}(k_2 - k_1)^\alpha \langle U_n^\alpha U_n^\beta \rangle (k_2 - k_1)^\beta] \times t_n(\vec{k}_2, \vec{k}_1) , \quad (1)$$

where $\vec{k}_1$ is the wave vector of the incident electron, $\vec{k}_2$ is the wave vector of the scattered electron, α and β are Cartesian indices and we use the convention of summing over repeated Cartesian indices, $\vec{U}_n$ is the displacement from equilibrium of the nth ion, $\langle\ \rangle$ denote a thermal ensemble average over the vibrational states of the solid, [4] and $t_n(\vec{k}_2, \vec{k}_1)$ is the scattering amplitude for the nth ion core when it is held rigid. To carry out an explicit evaluation of the scattered intensity, it is necessary to decompose the b_n into partial-wave components. As before, we will use a Debye model to characterize the vibrational properties of the ion cores, [5] i. e., we assume that each ion core has a spherically symmetric mode of vibration, the amplitude of which is parametrized by a Debye temperature. Using this approximation,

$$\tfrac{1}{2}(k_2 - k_1)^\alpha \langle U_n^\alpha U_n^\beta \rangle (k_2 - k_1)^\beta = W(T, \Theta_D^n, M)(\vec{k}_2 - \vec{k}_1)^2 , \quad (2)$$

where

$$W(T, \Theta_D^n, M_n) = \frac{3\hbar^2}{2M_n k_B \Theta_D^n} \times \left[\frac{1}{4} + \left(\frac{T}{\Theta_D^n} \right)^2 \int_0^{\Theta_D^n/T} dx\, \frac{x}{e^x - 1} \right] . \quad (3)$$

In Eq. (3), T is the temperature of the solid, M_n is the mass of the nth ion core, and Θ_D^n is the parameter describing the vibrational amplitude of the nth ion core.

The renormalization due to the lattice vibrations can appreciably change the angular dependence of the electron–ion-core scattering amplitude and can greatly increase the number of partial waves needed to describe $b_n(\vec{k}_2, \vec{k}_1)$. Suppose, for example, it takes l' partial waves to describe the angular dependence of the vibronic renormalization factor, i. e.,

$$\exp[-(\vec{k}_2 - \vec{k}_1)^2 W(T, \Theta_D^n, M_n)] = \sum_{l=0}^{l'} W_l(k, T, \Theta_D^n, M_n) P_l(\cos\theta_{12}) , \quad (4)$$

where θ_{12} is the angle between $\vec{k}_1$ and $\vec{k}_2$, and $k = |\vec{k}_1| = |\vec{k}_2|$. The value of l' needed in this expansion depends upon Θ_D^n, M_n, T, and the energy of the electron. The more sharply peaked this quantity is about $\theta_{12} = 0$, the more partial waves will be needed for this expansion. As a practical matter for the parameters used in this work, we need to have l' at least equal to 2. $t_n(\vec{k}_2, \vec{k}_1)$ is also expressed in terms of partial-wave components. These are obtained from a model of the electron–ion-core interaction potential. Suppose that it takes l'' partial waves to adequately describe this part of the interaction, i. e.,

$$t_n(\vec{k}_2, \vec{k}_1) = \sum_{l=0}^{l''} t_n^l(k) P_l(\cos\theta_{12}) . \quad (5)$$

Since $b_n(\vec{k}_2, \vec{k}_1)$ is the product of the quantities given in Eqs. (4) and (5), a partial-wave decomposition of it would require

$$\bar{l} = l' + l'' \quad (6)$$

partial waves. Using Snow's potential [29] to describe the electron–ion-core interaction, we need l'' at least equal to 2 to accurately model $t_n(\vec{k}_2, \vec{k}_1)$ for aluminum in the energy range under consideration. [19,22] It thus requires at least $\bar{l} = 4$ partial-wave components to accurately model the renormalized scattering amplitude. Unfortunately, the computer code available to us at the present time has only the capability of using $l \leq 2$ partial waves, and so we are forced into compromising either our model of $t_n(\vec{k}_2, \vec{k}_1)$ or the vibronic renormalization factor. This problem did not come up in earlier work [19,22] on aluminum which was compared with experimental data taken at only room temperature. [30–33] The relatively large value of $\Theta_D^n = 426°$ used in the theoretical calculations [19,22] also helped to make the vibronic renormalization factor not too sharply peaked in the forward scattering direction, and this reduced the number of partial-wave components needed to describe this part of the effective elastic scattering vertex.

In Ref. 5 it was shown that the effective Debye temperature obtained from the temperature dependence of the LEED intensity profiles generally lay between the Debye temperatures describing the vibrational amplitudes of the bulk and surface ion cores. The $\Theta_D^{\rm eff}(E)$ establish a "trend line" which shows the $\Theta_D^{\rm eff}(E)$ increasing to the bulk Θ_D with increasing E. Multiple scattering effects can introduce about a 15% fluctuation about this "trend line." For the Debye temperature parametrizing the vibrational amplitude of the bulk ion cores, we take

$$\Theta_D^B = 380\,°\mathrm{K} . \quad (7a)$$

This is in accord with the work of Flinn and McManus [34] which shows Θ_D for aluminum at $T \gtrsim 300\,°\mathrm{K}$ lying in the range (380–390) °K for both x-ray and heat-capacity measurements. We will use this value of Θ_D^B instead of the value [35] $\Theta_D^B = 426\,°\mathrm{K}$ which was used in Ref. 5. From the work of Quinto *et al.*, [28] we see that we must have

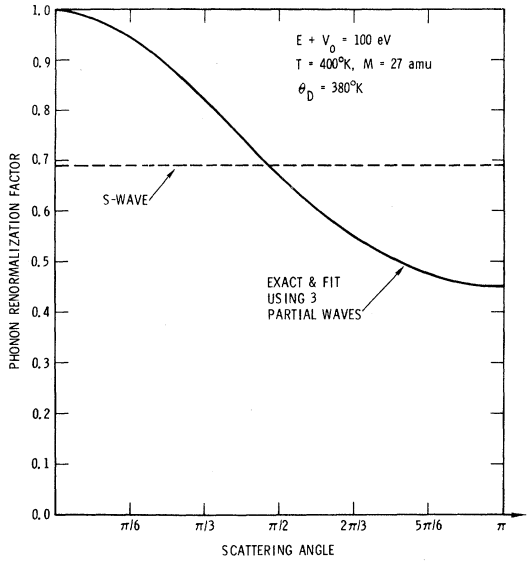

FIG. 1. Plot of the phonon renormalization factor for the electron–ion-core elastic scattering vertex as a function of scattering angle. The renormalization factor which is shown as the solid line was calculated using the Debye model for the ion-core vibration and the parameters shown in the figure. The s-wave approximation to the renormalization factor is shown as the horizontal dashed line. The approximation using three partial waves is indistinguishable from the exact result.

$$\Theta_D^S \lesssim 189\,^\circ\mathrm{K}\,, \tag{7b}$$

and so we take $\Theta_D^S = 180\,^\circ$K for the Debye temperature parametrizing the vibrational amplitude of the surface ion cores. The only theoretical calculations of the vibrational amplitude of the surface atoms are based upon two-body central force models to describe the interaction between the ion cores.[36–40] These calculations show that the vibrational amplitude of the ion cores falls off very quickly to the bulk vibrational amplitude with increasing distance from the surface. It is not clear to what extent these calculations apply to metals, but we shall first consider the case where *only* the surface ion cores have a vibrational amplitude different from the bulk value. Taking $\Theta_D^S = 180\,^\circ$K and $\Theta_D^B = 380\,^\circ$K means that in the high-temperature limit the surface atoms have a mean square vibrational amplitude about 4.4 times as large as the bulk ion cores. This is not an unreasonable figure compared with the results of the theoretical calculations.[36–40]

The final quantity that we need to specify for our calculation is the electron self-energy which we take as[5,19,22,25,26,41]

$$\Sigma(E) = -V_0 - i\Gamma(E)\,, \tag{8}$$

where

$$\Gamma(E) = (\hbar^2/m\lambda_{ee})\,[(2m/\hbar^2)\,(E+V_0)]^{1/2}\,. \tag{9}$$

In Eqs. (8) and (9) E is the energy of the electron outside the crystal, λ_{ee} is twice the inelastic-collision mean free path, and V_0 is the inner potential which for aluminum[5,19,22] we take as 16.7 eV.

III. NUMERICAL RESULTS

In Fig. 1, we show a plot for a bulk ion core of the vibronic renormalization factor given in Eq. (4) as a function of scattering angle for $T = 400\,^\circ$K and $E + V_0 = 100$ eV. The s-wave approximation to the renormalization factor

$$e^{-(\vec{k}_2-\vec{k}_1)^2}\,W(T,\Theta_D,M) \to W(k;T,\Theta_D,M)\,, \tag{10}$$

where

$$W(k;T,\Theta_D,M) = e^{-2Wk^2}(\sinh 2Wk^2)/2Wk^2 \tag{11}$$

and

$$W \equiv W(T,\Theta_D,M) \tag{12}$$

is shown as the horizontal dashed line in Fig. 1.

We first consider the situation where we use the $l = 0$, 1, 2 phase shifts[19,22] from Snow's potential[29,42] to describe the electron–rigid-ion scattering amplitude defined in Eq. (5) and use the s-wave part of the vibronic renormalization factor to describe the effect of the lattice vibrations. This is the procedure used by Tong and Rhodin.[18] An example of an intensity profile calculated using this model of the electron–ion-core vertex is shown in Fig. 2.

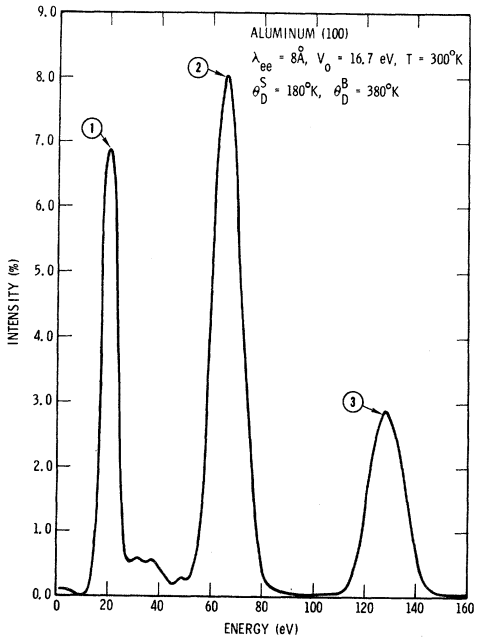

FIG. 2. Calculated intensity profile for the specular beam using the $l = 0, 1, 2$ phase shifts from Snow's potential (Ref. 29) and the s-wave approximation to the vibronic renormalization factor. The calculation is for a normally incident beam and uses the parameters indicated in the figure. The primary "Bragg" peaks are labeled for identification purposes.

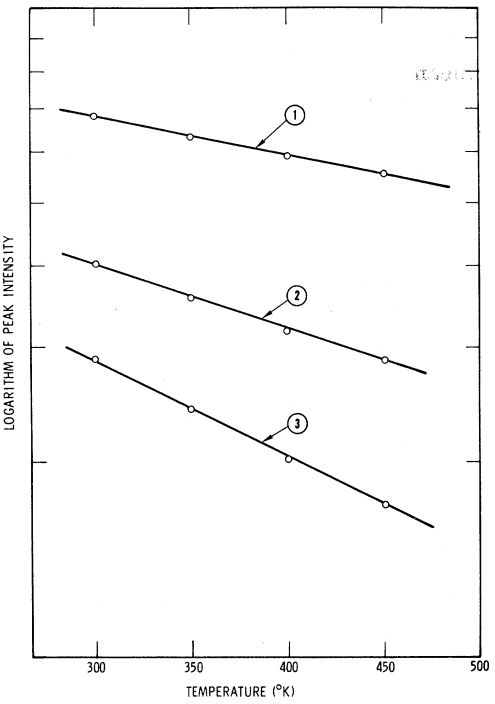

FIG. 3. Plot of the logarithm of peak intensity vs temperature for the peaks shown in Fig. 2. The intensity units are arbitrary.

The electronic parameters are the same as used in previous work,[19,22] but note that the secondary structure of the profile in Fig. 2 is greatly reduced relative to the secondary structure obtained in the previous calculations.[19,22] The secondary structure is fairly prominent in the experimental data[28,30,31] and so the calculation does not correctly reproduce this feature of the data. This is at least partially due to the use of the s-wave approximation for the vibronic renormalization factor. If the angular dependence of this factor were correctly described, then the forward scattering contribution of the surface atoms ($\theta_{12} \simeq 0$) would not be diminished by the vibrational motion (no matter how large the vibrational amplitude) and then secondary structure could result from multiple scattering between the surface atomic layer and the bulk atomic layers. Using $\Theta_D^S = 180\,^\circ\mathrm{K}$ and the s-wave approximation to the vibronic renormalization factor reduces the forward scattering component of the surface too much to allow enough of this multiple scattering to occur. When a substantially larger value of Θ_D^S is used,[18,20] this scattering is not too greatly reduced and secondary structure is seen in the calculated profiles. We consider next the primary Bragg peaks which superficially appear to be correctly described by this model.

To obtain an effective Debye temperature we simply see how the peak intensity changes with the temperature of the solid. We neglect any anomalous thermal expansion in the surface region but take the bulk lattice parameter for aluminum appropriate to the solid temperature.[43] The effective Debye temperatures are obtained by plotting the logarithm of peak intensity vs temperature as is shown in Fig. 3. In the kinematical approximation the intensity of a "Bragg" peak is assumed to behave like

$$I = I_0 \exp[-2W(T, \Theta_D^{\mathrm{eff}}, M)\,(\vec{k}_f - \vec{k}_i)^2]\,, \tag{13}$$

where in the high-temperature limit

$$W(T, \Theta_D, M) \to 3\hbar^2 T / 2Mk_B\Theta_D^2\,. \tag{14}$$

Using the input inner potential of 16.7 eV, we obtain the values of Θ_D^{eff} shown in the $\lambda_{ee} = 8$ Å column of Table II. Note that there is a substantial energy dependence to these Θ_D^{eff} with $\Theta_D^{\mathrm{eff}}(E)$ increasing as E increases. The energies of the peaks are measured external to the crystal. These are somewhat lower than the experimental peak positions which are given in Table I. Part of this shift is due to the fact that the experimental curves are for an angle of incidence of 5° while the theoretical curves are for a normally incident beam.

Effective Debye temperatures were obtained in the same way for $\lambda_{ee} = 4$ Å using the same vibronic parameters and those are also shown in Table II. Note that although the Θ_D^{eff} increase with increasing peak energy, the values are much too large when compared with the experimental values in Table I. The Θ_D^{eff} for the $n = 3$ and 4 Bragg peaks are even larger than Θ_D^B. This discrepancy is due to the use of the s-wave approximation to the vibronic renormalization factor. The origin of the difficulty can readily be seen on inspection of Fig. 1. Single scattering events make a significant

TABLE II. Effective Debye temperatures obtained from a model calculation which describes the effective electron–ion-core elastic scattering vertex by using the $l = 0, 1, 2$ phase shifts from Snow's potential (Refs. 29 and 42) and the s-wave approximation to the vibronic renormalization factor. Parameters of the calculation are $\Theta_D^S = 180\,^\circ\mathrm{K}$, $\Theta_D^B = 380\,^\circ\mathrm{K}$, $V_0 = 16.7$ eV with the geometrical parameters corresponding to Al(100).

[a]Peak	Energy[a] (eV)	$\lambda_{ee} = 4$ Å (°K)	$\lambda_{ee} = 8$ Å (°K)
1 ($n = 2$ Bragg peak)	19	307	380
2 ($n = 3$ Bragg peak)	65	401	450
3 ($n = 4$ Bragg peak)	127	473	491

[a]Peak position used in determining effective Debye temperature (position at 400 °K).

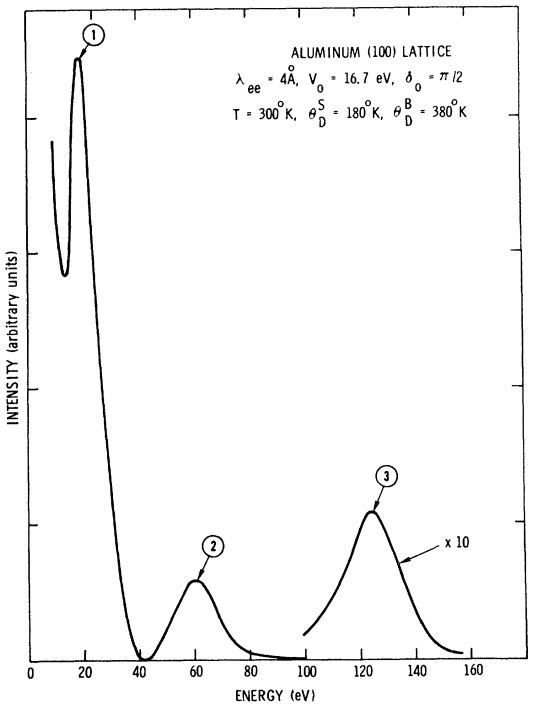

FIG. 4. Calculated intensity profile for the specular beam using the constant-phase-shift isotropic scatterer model for the rigid ion scattering amplitude (Refs. 25 and 26). The calculation is for a normally incident beam and uses the parameters indicated in the figure. The primary "Bragg" peaks are labeled for identification purposes.

contribution to the "Bragg" peak intensities and considering specular reflection of a normally incident beam, these events correspond to a scattering angle of $\theta_{12}=\pi$. At this angle the true phonon renormalization factor is substantially smaller than the s-wave approximation. At a given temperature and beam energy the s-wave approximation for a given Θ_D corresponds to the $\theta_{12}=\pi$ value of the renormalization factor for a much larger Θ_D. The kinematical analysis of the temperature dependence of the scattered intensity thus gives rise, especially for large-angle scattering, to Θ_D^{eff} that are erroneously large. The use of this approximation gives much too weak a temperature dependence for the "Bragg" peak intensities for large-angle scattering. Hence, the s-wave approximation for the vibronic renormalization factor does not quantitatively describe the behavior of either the primary or the secondary peaks in the intensity profiles.

Let us next consider the other limiting case where we use a simple constant-phase-shift s-wave model to describe the scattering properties of the rigid-ion core and accurately describe the vibronic renormalization factor. The electron–rigid-ion scattering amplitude is thus taken as[5,25,26,41]

$$t_n(\vec{k}_2,\vec{k}_1)=t_n(k)=(\pi i\hbar^2/mk)\,(e^{2i\delta_n}-1)\,, \tag{15}$$

where we use $\delta_n=\frac{1}{2}\pi$ for both the surface and the bulk atoms. This keeps the rigid-ion scattering properties of the surface and the bulk-ion cores the same. The vibronic renormalization factor is then written as

$$e^{-(\vec{k}_1-\vec{k}_2)^2W}\simeq e^{-2k^2W}[A_0P_0(\cos\theta_{12})+A_1P_1(\cos\theta_{12}) +A_2P_2(\cos\theta_{12})]\,. \tag{16}$$

Equating the left- and right-hand sides of Eq. (16) at $\theta_{12}=0$, $\frac{1}{2}\pi$, and π, we obtain

$$A_0=\tfrac{1}{3}(\cosh 2k^2W+2)\,, \tag{17a}$$

$$A_1=\sinh 2k^2W\,, \tag{17b}$$

$$A_2=\tfrac{2}{3}(\cosh 2k^2W-1)\,. \tag{17c}$$

For the parameters used in Fig. 1 the fit using Eqs. (17) was indistinguishable from the exact result. The differences between the left- and right-hand sides of Eq. (16) are not appreciable for any of the parameters used in this paper.

An example of an intensity profile calculated using Eqs. (15) and (16) to describe the effective electron–ion-core elastic scattering vertex is shown in Fig. 4. This calculated intensity profile exhibits the characteristic failings of the constant-phase-shift s-wave model[25,26] in that (a) only the primary "Bragg" peaks are described in an approximately correct way, (b) the calculated reflectivity diverges as $E\to 0$, and (c) the higher-energy "Bragg" peaks are greatly reduced in intensity relative to the lower-energy "Bragg" peaks. Nevertheless this simple model describes the temperature dependence of the "Bragg" peak intensities well enough to provide some insight into the experimental measurements.

In Fig. 5, we show a plot of the logarithm of peak intensity vs temperature for the peaks in Fig. 4. The values of Θ_D^{eff} obtained from these slopes are shown in the $\lambda_{ee}=4$ Å column of Table III. Effective Debye temperatures were obtained in the same way for $\lambda_{ee}=2$ and 8 Å for the same vibronic parameters, and these are also shown in Table III. The positions of the "Bragg" peaks are somewhat lower than those listed in Table II. Using this model the Θ_D^{eff} lie between Θ_D^S and Θ_D^B as expected. For a given λ_{ee} the Θ_D^{eff} exhibit a pronounced energy dependence with the Θ_D^{eff} increasing with increasing energy. This is because the vibrationally renormalized scattering amplitude of the surface atoms decreases relative to the vibrationally renormalized scattering amplitude of the bulk atoms with increasing electron energy. Thus, the relative surface-to-bulk contribution to the scattered intensity decreases with increasing electron

energy and we see a Θ_D^{eff} changing from a value more characteristic of the surface to a value more characteristic of the bulk.

Just as in Ref. 5, there is a strong dependence of Θ_D^{eff} for a given peak on λ_{ee} with Θ_D^{eff} moving closer to Θ_D^B with increasing λ_{ee}. Even for λ_{ee} as small as 4 Å, the calculated Θ_D^{eff} are larger than their experimental counterparts with a $\lambda_{ee}(E)$ between 2 and 4 Å being indicated for energies near the $n=4$ Bragg peak. One might be tempted to allow λ_{ee} to be energy dependent and obtain values for it by fitting to the observed Θ_D^{eff}. However, this is only valid to the extent that the vibrational properties of the ion cores in the surface region are known. To illustrate this we consider the situation where the surface ion cores are characterized by $\Theta_D^S = 180\,^\circ$K, the ion cores in the second layer are characterized by $\Theta_D^{(2)} = 280\,^\circ$K, and the ion cores in the remaining layers are characterized by the bulk value $\Theta_D^B = 380^\circ$. Effective Debye temperatures for the peaks in this case are shown in Table IV. Comparing corresponding Θ_D^{eff} between Tables III and IV shows that the shape of the profile for the decay of the vibrational amplitude to the bulk value can appreciably affect the values of $\Theta_D^{eff}(E)$. Comparing Tables I and IV still indicates $\lambda_{ee} < 4$ Å for $E \simeq 60$ eV but gives the possibility of 4 Å $< \lambda_{ee} <$ 8 Å for $E \simeq 120$ eV. One thing that should also be noticed is that the calculated Θ_D^{eff} for the $n=2$ Bragg peak are *higher* than the experimental value even though Θ_D^S is $\sim 10^\circ$ *lower* than the experimental value. This indicates that the lowest experimental Θ_D^{eff} provides an upper bound to Θ_D^S and hence gives a lower bound to the vibrational amplitude of the surface atoms. The particular Θ_D^S needed to give $\Theta_D^{eff} = 189\,^\circ$K for the $n=2$ "Bragg" peak will depend both on λ_{ee} and on the shape of the profile for the decay of the surface vibrational amplitude to the bulk value. We will not further pursue the problem of the determining $\lambda_{ee}(E)$ and Θ_D^S using this model but will wait until it is possible to accurately model *both* the rigid-ion scattering properties and the vibronic renormalization factor.

The measured $\Theta_D^{eff}(E)$ do seem to indicate a fairly small value for λ_{ee} and, if we were to take $\lambda_{ee} \simeq 4$ Å for $E + V_0 \simeq 75$ eV (which is certainly consis-

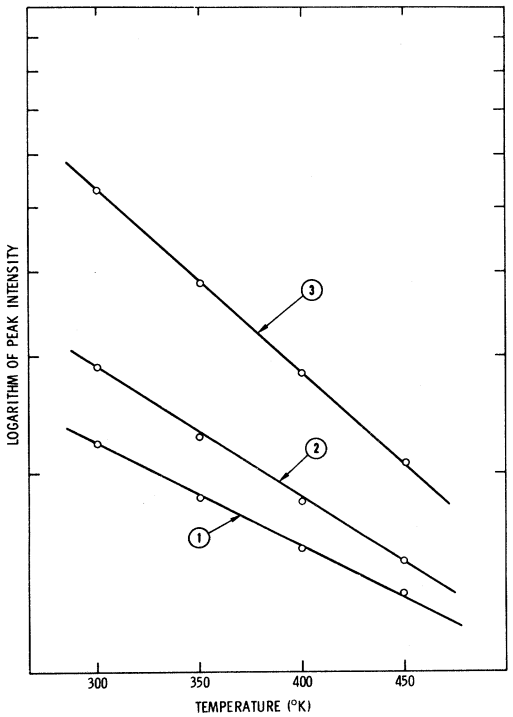

FIG. 5. Plot of the logarithm of peak intensity vs temperature for the peaks shown in Fig. 4. The intensity units are arbitrary.

TABLE III. Effective Debye temperatures obtained from a model calculation which accurately describes the vibronic renormalization of the electron–ion-core scattering amplitude but uses only s waves to describe the scattering properties of a rigid ion core. Parameters of the calculation are $\Theta_D^S = 180\,^\circ$K, $\Theta_D^B = 380\,^\circ$K, $\delta_0 = \frac{1}{2}\pi$, $V_0 = 16.7$ eV with the geometrical parameters corresponding to Al (100).

Peak	Energy[a] (eV)	$\lambda_{ee}=2$ Å (°K)	$\lambda_{ee}=4$ Å (°K)	$\lambda_{ee}=8$ Å (°K)
1	17	b	235	304
($n=2$ Bragg peak)				
2	60	233	307	352
($n=3$ Bragg peak)				
3	123	304	354	367
($n=4$ Bragg peak)				

[a]Peak position used in determining effective Debye temperature (position at 400 °K).

[b]The reflectivity boundary conditions wash out the first peak for this set of parameters.

TABLE IV. Effective Debye temperatures obtained from a model calculation which accurately describes the vibronic renormalization of the electron–ion-core scattering amplitude but uses only s waves to describe the scattering properties of a rigid ion core. Parameters of the calculation are $\Theta_D^S = 180\,^\circ$K, $\Theta_D^{(2)} = 280\,^\circ$K, $\Theta_D^B = 380\,^\circ$K, $\delta_0 = \frac{1}{2}\pi$, $V_0 = 16.7$ eV with the geometrical parameters corresponding to Al (100).

Peak	Energy[a] (eV)	$\lambda_{ee}=4$ Å (°K)	$\lambda_{ee}=8$ Å (°K)
1	17	220	276
($n=2$ Bragg peak)			
2	60	262	316
($n=3$ Bragg peak)			
3			
($n=4$ Bragg peak)	123	306	338

[a]Peak position used in determining effective Debye temperature (position at 400 °K).

tent with the experimental results), this would give $\mathrm{Im}\Sigma \simeq 8.5$ eV. This is substantially larger than the values given by bulk electron gas calculations[44,45] which are in the range 3–5 eV. This difference could be due to surface plasmon losses which are comparable to bulk plasmon losses.[46,47] $\lambda_{ee} \simeq 4$ Å is, however, in agreement with the values of the inelastic mean free path obtained from photoemission work in aluminum for electrons above the bulk plasmon threshold.[48]

IV. SUMMARY

In summary, we have discussed the effect of lattice vibrations in renormalizing the effective electron–ion-core elastic scattering. It was not possible to accurately treat the renormalized electron–ion-core elastic scattering amplitude using the computer codes presently available to us so we considered instead the two limiting models for the renormalized vertex. One limit involved accurately describing the rigid-ion part of electron–ion-core scattering amplitude but using only the s-wave portion of the vibronic renormalization factor. It was found that this procedure did not accurately describe the behavior of the temperature dependence of either the primary or the secondary structure in the intensity profiles. The other limit that was studied involved using an s-wave model to describe the rigid-ion scattering and accurately treating the vibronic renormalization factor. Although totally inadequate for the secondary structure this approach appeared to at least semiquantitatively describe the behavior of the primary "Bragg" peaks in the intensity profiles. We note in passing that if one is only interested in describing the qualitative features of the experimental data, this can often be done using only s waves for both the rigid-ion scattering and the vibronic renormalization factor.[49] We obtained effective Debye temperatures by kinematically parametrizing the temperature dependence of the "Bragg" peaks. Even though a constant inelastic-collision mean free path was used in the calculation, it was found that the Θ_D^{eff} for the Bragg peaks exhibited a significant energy dependence. This was due simply to the temperature-dependent renormalization of the electron–ion-core elastic cross section reducing the cross section for the surface atoms much more with increasing energy than for the bulk atoms, which was a consequence of the larger amplitude of vibration of the surface atoms. It was found that Θ_D^{eff} depended quite sensitively on the form of the falloff of the surface vibrational amplitude with distance from the surface. The lowest Θ_D^{eff} for the peaks in the intensity profile always lay above the value of Θ_D^S, indicating that the lowest Θ_D^{eff} provides an upper bound on Θ_D^S. By comparing the calculated Θ_D^{eff} with the experimental measurements of Quinto *et al.*[28] a crude estimate of $\mathrm{Im}\Sigma$ was obtained. This was substantially higher than the results of bulk electron gas calculations[44,45] which did not include the effects of surface plasmons, but are in agreement with estimates reported by Ritchie[48] from photoemission work in aluminum.

---

*Work supported by the U. S. AEC.

[1]M. Born, Rept. Progr. Phys. 9, 294 (1942).

[2]C. Kittel, *Quantum Theory of Solids* (Wiley, New York, 1963), Chap. 19.

[3]C. Kittel, *Introduction to Solid State Physics* (Wiley, New York, 1963), Chap. 6.

[4]C. B. Duke and G. E. Laramore, Phys. Rev. B 2, 4765 (1970).

[5]G. E. Laramore and C. B. Duke, Phys. Rev. B 2, 4783 (1970).

[6]A. U. McRae and L. H. Germer, Phys. Rev. Letters 8, 489 (1962).

[7]A. U. McRae, Surface Sci. 2, 522 (1964).

[8]E. R. Jones, J. T. McKinney, and M. B. Webb, Phys. Rev. 151, 476 (1966).

[9]J. T. McKinney, E. R. Jones, and M. B. Webb, Phys. Rev. 160, 523 (1967).

[10]R. M. Goodman, H. H. Farrell, and G. A. Somorjai, J. Chem. Phys. 48, 1046 (1968).

[11]J. M. Morabito, Jr., R. F. Steiger, and G. A. Somorjai, Phys. Rev. 179, 638 (1969).

[12]D. P. Woodruff and M. P. Seah, Phys. Letters 30A, 263 (1969).

[13]S. Andersson and B. Kasemo, Solid State Commun. 8, 1885 (1970).

[14]D. Tabor and J. Wilson, Surface Sci. 20, 203 (1970).

[15]D. Tabor, J. M. Wilson, and T. J. Bastow, Surface Sci. 26, 471 (1971).

[16]J. A. Strozier, Jr. and R. O. Jones, Phys. Rev. Letters 25, 516 (1970).

[17]J. A. Strozier, Jr. and R. O. Jones, Phys. Rev. B 3, 3228 (1971).

[18]S. Y. Tong and T. N. Rhodin, Phys. Rev. Letters 25, 711 (1971).

[19]G. E. Laramore, C. B. Duke, A. Bagchi, and A. B. Kunz, Phys. Rev. B 4, 2058 (1971).

[20]D. W. Jepsen, P. M. Marcus, and F. P. Jona, Phys. Rev. Letters 26, 1365 (1971); Phys. Rev. B5, 3933 (1972).

[21]J. B. Pendry, Phys. Rev. Letters 27, 856 (1971).

[22]G. E. Laramore and C. B. Duke, Phys. Rev. B 5, 267 (1972).

[23]J. S. Schilling and M. B. Webb, Phys. Rev. B 2, 1665 (1970).

[24]F. Herman and S. Skillman, *Atomic Structure Calculations* (Prentice-Hall, Englewood Cliffs, N. J., 1963).

[25]C. B. Duke, J. R. Anderson, and C. W. Tucker, Jr., Surface Sci. 19, 117 (1970).

[26]C. W. Tucker, Jr. and C. B. Duke, Surface Sci. 24, 31 (1971).

[27]In the strictest sense when multiple scattering is present, one cannot speak of Bragg peaks. The kinematical "Bragg" condition is reflected in the intensity

profiles only as an envelope for the multiple scattering peaks. This point is discussed in some detail in Ref. 26. However, in a weak scattering material such as aluminum, there are prominent peaks near the kinematical "Bragg" positions, and we shall, following the usual nomenclature, refer to these as "Bragg" peaks.

[28]D. T. Quinto and W. D. Robertson, in Proceedings of the International Conference on Solid Surfaces (unpublished); and D. T. Quinto, B. W. Holland, and W. D. Robertson, Surface Sci. (to be published).

[29]E. C. Snow, Phys. Rev. 158, 683 (1967).

[30]H. H. Farrell and G. A. Somorjai, Phys. Rev. 182, 751 (1969).

[31]F. Jona, IBM J. Res. Develop. 14, 444 (1970).

[32]J. M. Burkstrand and F. M. Propst, J. Vac. Sci. Technol. 9, 731 (1972).

[33]J. O. Porteus and W. N. Faith, in Proceedings of the Fifth Low-Energy–Electron-Diffraction Seminar, 1971 (unpublished); J. Vac. Sci. Technol. 9, 1062 (1972).

[34]P. A. Flinn and G. M. McManus, Phys. Rev. 132, 2458 (1963).

[35]The value $\Theta_D^B = 426°$ corresponds to the results of a low-temperature specific-heat measurement. See R. C. Weast, S. M. Selby, and C. D. Hodgman, *Handbook of Chemistry and Physics*, 46th ed. (Chemical Rubber, Cleveland, 1965), p. D-86.

[36]M. Rich, Phys. Letters 4, 153 (1963).

[37]A. A. Maradudin and J. Melgailis, Phys. Rev. 133, A1188 (1964).

[38]R. F. Wallis, B. C. Clark, and R. Herman, in *The Structure and Chemistry of Solid Surfaces*, edited by G. A. Somorjai (Wiley, New York, 1969), p. 17-1.

[39]R. E. Allen and F. W. deWette, Phys. Rev. 179, 873 (1969).

[40]R. E. Allen, F. W. deWette, and A. Rahman, Phys. Rev. 179, 887 (1969).

[41]C. B. Duke and C. W. Tucker, Jr., Phys. Rev. Letters 23, 1163 (1969).

[42]In obtaining the phase shifts from Snow's potential the energy zero was taken at the constant part of the muffin tin. However, the discontinuity in the potential at the muffin-tin radius was adjusted so as to fit the known values of the work function and the Fermi energy. This allows us to have a self-consistent definition of the energy zero for both the electron–ion-core potential and the electronic self-energy entering the electron propagator. An alternate procedure is used by Jepsen *et al.* (Ref. 20) who use Snow's value for the muffin-tin discontinuity and treat the real part of the electronic self-energy as a completely adjustable parameter. The phase shifts used in the present work are explicitly shown in Refs. 19 and 22. The s-wave phase shift in particular differs appreciably from that used by Jepsen *et al.*

[43]The measured thermal-expansion coefficient for bulk aluminum was used to determine the change in lattice constant with temperature. See A. Goldsmith, T. E. W Waterman, and H. J. Hirschhorn, *Handbook of Thermophysical Properties of Solid Materials* (McMillan, New York, 1961), Vol. I, p. 49.

[44]J. J. Quinn, Phys. Rev. 126, 1453 (1962).

[45]B. I. Lundquist, Phys. Status Solidi 32, 273 (1969).

[46]C. B. Duke and C. W. Tucker, Jr., Surface Sci. 15, 231 (1969).

[47]A. Bagchi and C. B. Duke, Phys. Rev. B 5, 2784 (1972).

[48]R. H. Ritchie, in Proceedings of the Fifth Low-Energy–Electron-Diffraction Seminar, 1971 (unpublished).

[49]B. W. Holland, Surface Sci. 28, 258 (1971).